

Regular article

Cluster modeling of metal oxides: case study of MgO and the CO/MgO adsorption system*

X. Xu^{1,2}, H. Nakatsuji^{2,3}, X. Lu¹, M. Ehara², Y. Cai¹, N.Q. Wang¹, Q.E. Zhang¹

¹ State Key Laboratory for Physical Chemistry of Solid Surfaces, Institute for Physical Chemistry, Department of Chemistry, Xiamen University, Xiamen 361005, China

² Department of Synthetic Chemistry and Biochemistry, Faculty of Engineering, Kyoto University, Kyoto 606-8501, Japan

³ Institute for Fundamental Chemistry, 34-4, Takano-Nishihiraki-cho, Sakyo-ku, Kyoto 606-8103, Japan

Received: 26 June 1998 / Accepted: 17 September 1998 / Published online: 23 February 1999

Abstract. Three principles, namely, a neutrality principle, a stoichiometry principle, and a coordination principle are proposed as criteria for building up cluster models of metal oxides. Particular attention is focused on how to cut out a stoichiometric cluster which possesses the smallest boundary effect for a given cluster size. Several criteria for determining self-consistently the magnitudes of embedding point charges are discussed. The problem of how the methods of embedding affect the calculated electronic properties of the substrate cluster and the adsorption properties are investigated. It is that a better cutout cluster, which interacts less with its surroundings, would depend less on the embedding scheme, while a better description of the surroundings would improve the quality of the cutout cluster. A simple point charge model provides a stable model of the oxide surface as well as of adsorption on the surface.

Key words: Cluster model – Ab initio – Metal oxide – MgO – CO adsorption

1 Introduction

Metal oxides form a class of systems with important applications in, for example, catalysis, corrosion, gas sensors, ceramics, high-temperature superconductivity, etc. [1, 2]. In catalysis, oxides are commonly used either as support materials or as catalytically active components. To elucidate the nature of the oxide surfaces is very important to understand the catalytic reactivity of the oxide. Nowadays, theoretical modeling of the atomic details of surface structures and surface reactions has become a valuable tool which complements experimental surface science techniques [3, 4].

There are three popular methods for cluster modeling of metal oxides, i.e., the bare-cluster model, the embedded-cluster model, and the saturated-cluster model [5, 6]. The bare-cluster model is simply a small portion of substrate atoms cut out from the bulk solid. In the saturated-cluster model, hydrogens, pseudo-hydrogens, or some other atoms are used to saturate the free valencies at those sites of the bare cluster which are not supposed to represent the real solid, while in the embedded-cluster model, high-level quantum mechanical (QM) methods are applied to the cluster with its surroundings being treated at a lower level. Some sophisticated embedding schemes have been developed [7–13]. Among them, the hybrid QM/molecular mechanical (MM) method seems promising, where the surroundings are approximated by the MM model [11, 12]. At present, the most common, yet most effective way is to simulate the influence of the surroundings with a point charge (PC) array which adopts the lattice position of the bulk solid.

The bare-cluster model reduces the problem of an infinite solid to the common problem of molecules, and hence standard and well-documented ab initio computational methods for molecules can be used to explore the properties of solids and the chemistry on surfaces. However, the simulation with bare clusters can only be justified if the structures of the stable clusters and of the bulk are similar. The embedded-cluster model or the saturated-cluster model should be superior to the bare-cluster model, since the influence of the bulk solid has more or less been taken into account. It is clear, however, that a crude procedure for cutting out a cluster from the solid will create spurious electronic states at the border of the cluster which are hard to correct in the subsequent embedding or saturation. Cutting out a cluster suitably is a prerequisite for a good cluster modeling of a solid. How to cut out a cluster model is the first question we want to address in this paper.

It is generally believed that the embedded-cluster model with PCs is more suitable for modeling an ionic oxide where the orbital overlaps and orbital interactions are smaller, while the saturated-cluster model is better for

*Contribution to the Kenichi Fukui Memorial Issue

Correspondence to: X. Xu
e-mail: xinxu@xmu.edu.cn

a covalent oxide in which the dangling bonds are eliminated by saturators, such as hydrogens. In fact, on the one hand, hydrogens would be located at lattice sites so as to fulfill the “geometric requirements” of the bulk (the “electronic requirement” can hardly be fulfilled owing to the differences in the electronic properties between hydrogens and the lattice atoms which the hydrogens are going to replace); on the other hand, the embedded-cluster model with PCs, which can give a reasonably good description of an ideal ionic surface, would, however, result in an overestimation of the electrostatic interaction between the metal oxide surface and the polar adspecies. When the embedded-cluster model is used to study chemisorption, the replacement of lattice atoms with PCs would lead to a biased description of the stability of the ionic adspecies. Therefore, it is important to find a method which suitably accounts for the effects of the lattice field. What is more, since most metal oxides are intermediates between purely ionic and purely covalent solids, it is important to develop embedding techniques which can be applied to the modeling of an ordinary metal oxide. In this paper, we will try to address the question of how to suitably account for the cluster-lattice interaction within the PC embedding model.

The outline of the paper is as follows. In Sect. 2, we present three principles for building up cluster models of metal oxides. Particular attention is focused on how to cut out a stoichiometric cluster which possesses the smallest boundary effect for a given cluster size. The theoretical background of the embedded cluster model is discussed in Sect. 4. Several criteria for determining self-consistently the magnitudes of PCs are proposed. In Sect. 3 and 5, we present case studies for the cluster modeling of MgO solid and the CO/MgO (100) adsorption system to demonstrate our ideas. Some concluding remarks are made in Sect. 6.

2 Three principles for building up cluster models

The methods of modeling depend largely on the properties of the particular system in question. An oxide can be highly ionic, such as MgO, or significantly covalent, such as SiO₂. Many, for example, ZnO lie somewhere in-between. Indeed, oxides differ significantly from each other in such properties as crystal structure, electronic structure, etc. This fact makes it difficult to set up unified principles for the cluster modeling of oxides. Fortunately, there are some basic rules which all metal oxides should obey. These are the neutrality principle, the stoichiometry principle and the coordination principle [14, 15].

Possible cluster models for MgO are given in Table 1. In the MgO crystal, every Mg²⁺ has six nearest neighbor O²⁻. Therefore [MgO₆]¹⁰⁻ and [MgO₅]⁸⁻ are quite com-

mon models for the bulk solid and for the fivefold Mg site on the MgO (100) surface [13, 16–18]. Even though MgO has been generally accepted as a highly ionic oxide, there exist some arguments, from both experiment and theory, that the ionicity of MgO is significantly (10–20%) lower than the nominal value [19–21]. Keeping the stoichiometric ratio of MgO in mind, we have [Mg^{q+}(O^{q-})₆]^{5q-} for the solid and [Mg^{q+}(O^{q-})₅]^{4q-} for the surface; however, q is a quantity to be solved.

We believe the neutrality principle would be the most important. Though it is not uncommon to use a charge model to elucidate certain properties of oxide solids [22], this kind of model should be of limited value to investigate adsorption and surface reactions. A negative-charge model would be too active in donating electrons, while a positive-charge one would be eager to accept electrons. The unrealistic electric properties of such a charge model will artificially shift the energies of the frontier orbitals, and will create spurious static interaction with the adsorbate. Since the model is made up of “cluster + surroundings”, the neutrality principle would be fulfilled by a neutral cluster plus neutral surroundings, and by a charged cluster plus surroundings of the opposite charge (see Table 1). We think the former is superior to the latter, even though both models have found successful applications [3–6, 13, 16–18, 23, 24]. The reasons are:

1. The cluster should interact as little as possible with its surroundings [6], and the interaction between a neutral cluster and neutral surroundings should be smaller than that between a charged cluster and charged surroundings.
2. In a charged-cluster model, one has to ascribe a certain number of electrons to the cluster ion, usually based on the nominal ionicity of the substrate atoms, while the ionicity is a quantity in question [23].
3. The stoichiometry principle can never be fulfilled in a charged-cluster model, and the breaking down of the stoichiometry principle will bring about some artificial density of states of the excess atoms [24].

We recommend choosing a stoichiometric cluster [14, 15]. In this way, the neutrality requirement is reached automatically. The remaining question is how to minimize the boundary effect of a cluster of given size so as to fulfill the requirement of the coordination principle.

3 Modeling of MgO solid with bare stoichiometric (MgO)_x clusters

The MgO crystal has a rock-salt structure with a nearest Mg–O distance of 2.105 Å [25]. Each bulk Mg or O ion is coordinated by six counterions. The geometries of a set of stoichiometric (MgO)_x ($x = 1–16$)

Table 1. Sample clusters used to model MgO solid

| | Neutral cluster | Charged cluster |
|--------------------------|---|--|
| Bare model | (MgO) _x | (MgO ₆) ^{5q-} |
| Embedded model | (MgO) _x + (q ⁺ , q ⁻) | (MgO ₆) ^{5q-} + (q ⁺ , q ⁻) ^{5q+} |
| Hydrogen-saturated model | (MgO) _x + (H) _y | (MgO ₆) ^{5q-} + (H ⁺) _{5q} |


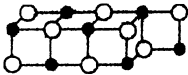

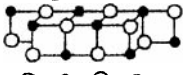
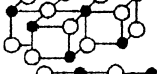
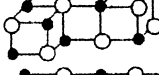
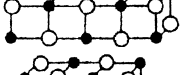
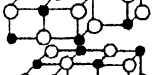
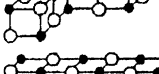
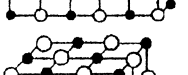
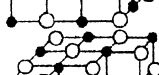
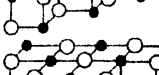
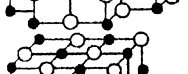
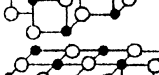

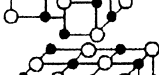
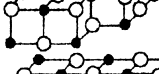
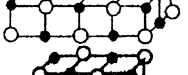
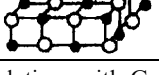
are presented in Table 2. These clusters are simply segments of the bulk. For a given x , there are a number of different choices to cut out a cluster. The model should work best if the boundary effect is the smallest. Cutting out a cluster would result in dangling bonds on

the border atoms of the cluster. We define N_d as the total number of dangling bonds of a cutout cluster, and $\beta_d = N_d/2x$ as the average number of dangling bonds on each in-cluster atom [14]. It is expected that for a given x , the cluster with the minimum N_d should have

Table 2. Ab initio RHF calculations for $(\text{MgO})_x$ clusters^a

| N | Cluster ^b | Symmetry | N_c | β_c | N_d | β_d | N_a | β_a | E_c (eV) ^c |
|----|----------------------|----------------|-------|-----------|-------|-----------|-------|-----------|-------------------------|
| 1a | | $C_{\infty v}$ | 2 | 1.0 | 10 | 5.0 | 10 | 5.0 | -2.21 |
| 2a | | $C_{\infty v}$ | 6 | 1.5 | 18 | 4.5 | 18 | 4.5 | -0.99 |
| 2b | | D_{2h} | 8 | 2.0 | 16 | 4.0 | 16 | 4.0 | 0.66 |
| 3a | | $C_{\infty v}$ | 10 | 1.67 | 26 | 4.33 | 26 | 4.33 | -0.12 |
| 3b | | C_s | 12 | 2.0 | 24 | 4.0 | 22 | 3.67 | 0.04 |
| 3c | | C_{2v} | 14 | 2.33 | 22 | 3.67 | 22 | 3.67 | 1.73 |
| 4a | | C_{2v} | 20 | 2.5 | 28 | 3.5 | 27 | 3.38 | 1.64 |
| 4b | | C_{2v} | 20 | 2.5 | 28 | 3.5 | 27 | 3.38 | 1.69 |
| 4c | | C_{2h} | 20 | 2.5 | 28 | 3.5 | 28 | 3.5 | 2.37 |
| 4d | | T_d | 24 | 3.0 | 24 | 3.0 | 24 | 3.0 | 3.11 |
| 5a | | C_{4v} | 26 | 2.6 | 34 | 3.4 | 26 | 2.6 | 0.32 |
| 5b | | C_{4v} | 26 | 2.6 | 34 | 3.4 | 30 | 3.0 | 1.16 |
| 5c | | C_1 | 30 | 3.0 | 30 | 3.0 | 28 | 2.8 | 2.69 |
| 5d | | C_{2v} | 26 | 2.6 | 34 | 3.4 | 34 | 3.4 | 2.73 |
| 6a | | C_{4v} | 30 | 2.5 | 42 | 3.5 | 26 | 2.17 | -0.61 |
| 6b | | C_{2h} | 32 | 2.67 | 40 | 3.33 | 40 | 3.33 | 2.98 |
| 6c | | D_{2h} | 40 | 3.33 | 32 | 2.67 | 32 | 2.67 | 3.83 |
| 7a | | C_s | 46 | 3.29 | 38 | 2.71 | 34 | 2.43 | 3.06 |
| 7b | | C_1 | 46 | 3.29 | 38 | 2.71 | 36 | 2.57 | 3.49 |
| 8a | | C_s | 52 | 3.25 | 44 | 2.75 | 40 | 2.5 | 3.13 |
| 8b | | C_s | 56 | 3.5 | 40 | 2.5 | 38 | 2.38 | 3.86 |

Table 2 (Contd.)

| N | Cluster ^b | Symmetry | N_c | β_c | N_d | β_d | N_a | β_a | E_c (eV) ^c |
|-----|---|----------|-------|-----------|-------|-----------|-------|-----------|-------------------------|
| 8c |  | D_{2d} | 56 | 3.5 | 40 | 2.5 | 40 | 2.5 | 4.21 |
| 9a |  | C_1 | 62 | 3.44 | 46 | 2.56 | 44 | 2.44 | 3.86 |
| 9b |  | C_{4v} | 66 | 3.67 | 42 | 2.33 | 42 | 2.33 | 4.43 |
| 10a |  | C_2 | 68 | 3.4 | 52 | 2.6 | 48 | 2.4 | 3.59 |
| 10b |  | C_2 | 72 | 3.6 | 48 | 2.4 | 44 | 2.2 | 3.89 |
| 10c |  | C_1 | 72 | 3.6 | 48 | 2.4 | 46 | 2.3 | 4.20 |
| 10d |  | D_{2h} | 72 | 3.6 | 48 | 2.4 | 48 | 2.4 | 4.44 |
| 11a |  | C_1 | 80 | 3.64 | 52 | 2.36 | 50 | 2.08 | 4.34 |
| 12a |  | C_s | 80 | 3.64 | 52 | 2.36 | 50 | 2.08 | 4.41 |
| 12b |  | D_{2d} | 88 | 3.67 | 56 | 2.33 | 56 | 2.33 | 4.59 |
| 12c |  | C_{2h} | 92 | 3.83 | 52 | 2.17 | 52 | 2.17 | 4.76 |
| 13a |  | C_s | 98 | 3.77 | 58 | 2.23 | 54 | 2.08 | 4.27 |
| 13b |  | C_s | 98 | 3.77 | 58 | 2.23 | 54 | 2.08 | 4.28 |
| 14a |  | C_2 | 108 | 3.86 | 60 | 2.14 | 56 | 2.0 | 4.44 |
| 14b |  | C_1 | 108 | 3.86 | 60 | 2.14 | 58 | 2.07 | 4.64 |
| 14c |  | C_1 | 108 | 3.86 | 60 | 2.14 | 58 | 2.07 | 4.68 |
| 15a |  | C_s | 118 | 3.93 | 62 | 2.07 | 60 | 2.14 | 4.75 |
| 15b |  | C_{2v} | 118 | 3.93 | 62 | 2.07 | 62 | 2.07 | 4.95 |
| 16a |  | D_{2d} | 128 | 4.0 | 64 | 2.0 | 64 | 2.0 | 5.05 |

^a RHF calculations with Gaussian 94 [27]. The basis sets are CEP-31[28] ^b Black dot: Mg atom; Circle: O atom

^c $E_c = E(\text{MgO}) - E[(\text{MgO})_x/x]$, where $E(\text{MgO})$ is the summation of the HF energies of atomic Mg(¹S) and O(³P); $E[(\text{MgO})_x/x]$ is the total energy of the $(\text{MgO})_x$ cluster divided by the size of the cluster, x

the smallest boundary effect and should be the most stable. Along with the increase in x , there are more and more inner atoms, the corresponding β_d should decrease, and the cluster should become closer and closer to the solid. Similarly, one may define N_c and $\beta_c = N_c/2x$, where N_c is the summation of the coordination number of each in-cluster atom and β_c denotes the average coordination number of an in-cluster atom. It is clear that as the size of the cluster increases, N_c and β_c should also increase [26]. In the perfect MgO bulk solid, β_c is equal to 6.0. For a covalent oxide, electrons would be well localized between atoms, while for an ionic oxide, electrons are believed to be well localized on atoms. So the geometry of an ionic oxide would be largely decided by the crystal field it experiences rather than by the bond direction as is most likely in a covalent oxide. Therefore, one may argue that for an ionic oxide like MgO, it is better to define N_a (or β_a), which counts up the total (or average) number of nearest neighbors missing in the cluster. It is anticipated that the best cluster model for a given x would correspond to the cluster with the smallest N_a for a given size. Table 2 summarizes the topologic parameters $N_d(\beta_d)$, $N_c(\beta_c)$ and $N_a(\beta_a)$. The cohesive energies, E_c , calculated with ab initio restricted Hartree–Fock (RHF) methods are also summarized in Table 2. A higher value of E_c indicates a more stable cluster.

Judging from the data in Table 2, we can make the following remarks:

1. $N_c(\beta_c)$ and $N_d(\beta_d)$ seem to work better than $N_a(\beta_a)$. The cluster with the largest N_c (the most saturated) and the smallest N_d (the fewest dangling bonds) is the most stable (the highest E_c) among those of the same size. From $x = 1$ to 16, β_c increases from 1.0 to 4.0, while β_d or β_a decreases from 5.0 to 2.0, indicating $(\text{MgO})_{16}$ is closer to the bulk than $(\text{MgO})_1$. All these are in general agreement with the ab initio calculations. While $N(N_c, N_d, \text{ or } N_a)$ provides a simple measure of the relative stability of clusters of the same size, $\beta(\beta_c, \beta_d \text{ or } \beta_a)$ measures the relative stability of clusters of different size. The oscillation of $N(\beta)$ with x clearly shows that the well-known boundary effect should be further divided into two effects, i.e., the size effect (dependence on the size of the cluster) and the shape effect (dependence on the shape of the cluster). A casually chosen larger cluster may even be a worse model for a solid or a surface than a carefully chosen smaller cluster, owing to the shape effect. The topological parameters N and β provide a simple way to keep the shape effect under control.

2. To maintain a high N_c or a low N_d (or N_a), cluster atoms with a coordination number less than 3 should be avoided. Actually, no atoms coordinated with fewer than three counterions exist in the real MgO solid or surfaces, even when the terrace-step-kink structures are taken into consideration. For sizes such as $x = 1, 2, 3, 5, \text{ or } 7$, cluster atoms with coordination numbers of 7 or 2 are unavoidable. Therefore these kinds of clusters would not be good models for MgO solid. This provides a simple way to exclude some cluster models from detailed consideration.

3. For a given x , there exist clusters of different shape but with the same N_c or N_d , for example, 8b and 8c, or 10b, 10c, and 10d, etc. Changing from 8c to 8b, two atoms increase their coordination numbers from 4 to 5, while the other two decrease their coordination numbers from 4 to 3. Therefore there are no net changes for N_c and N_d . In a perfect bulk solid, all Mg or O are equivalent to each other; hence we prefer a cluster with higher symmetry. Symmetry constraints helps to restrict atoms from being equivalent to each other. In fact, as shown by the data in Table 2, for a given x , the cluster with higher symmetry is always lower in energy.

4. For the rock-salt-type solid, the cubic model is preferred. 4d is the minimal cubic cluster. Additionally clusters such as 4d, 6c, 8c, 9b, 10d, 12c, 15b, 16a etc. should be better models than others of the same size to describe the respective surface active sites of interest. The convergence property of the calculated cohesive energies within the cubic $(\text{MgO})_x$ clusters is illustrated in Fig. 1. E_c increases smoothly as the size of the cluster increases. However, as shown by the data in Table 2, E_c would oscillate strongly with x if the shapes of the clusters were chosen arbitrarily. We have employed these cubic clusters to study O/MgO [29], NO/MgO [30], and $\text{N}_2\text{O}/\text{MgO}$ [31]. These clusters provided a convergent description of the reactivity of the respective surface-active sites.

All these observations clearly demonstrate the effectiveness of using the topological parameters $N(N_c, N_d, \text{ or } N_a)$ and $\beta(\beta_c, \beta_d, \text{ or } \beta_a)$ for guidance in cutting out clusters (cf. Fig. 1).

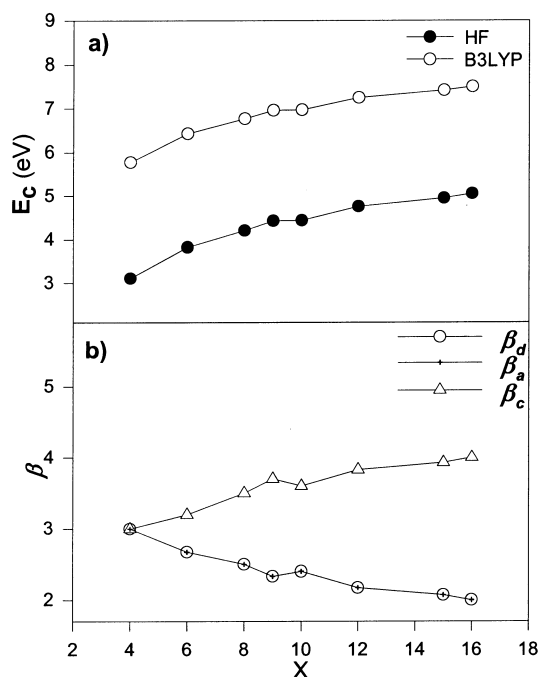


Fig. 1. a,b. Size dependence for the cubic $(\text{MgO})_x$ ($x = 4d, 6c, 8c, 9b, 10d, 12c, 15b, 16a$) clusters. **a** Convergence property of the calculated cohesive energies, E_c 's. Calculation results with B3LYP method [32, 33] are also presented; **b** Topological parameters β_c , β_d , and β_a as functions of cluster size, x

4 Embedding scheme within the PC model

Suppose the solid can be divided into two parts, i.e., a cutout cluster (index C) and its surroundings (index S). Neglecting the electron exchange between C and S, the zero-order wave function of bulk solid, Ψ_{bulk} , can be approximated in terms of Φ_C and Φ_S as a simple product, and the interaction energy E_{CS} can be given by the first-order correction from the direct electrostatic interaction [34]. When S is approximated by a PC array, the total energy of such an ideal system can be expressed as

$$E = \left\langle \Phi_C \left| \sum_{i \in C} T_i - \sum_{i \in C} \sum_{a \in C} \frac{Z_a}{r_{ia}} - \sum_{i \in C} \sum_{p \in S} \frac{Q_p}{r_{ip}} + \sum_{i > j \in C} \frac{1}{r_{ij}} \right| \Phi_C \right\rangle + \sum_{a > b \in C} \frac{Z_a Z_b}{R_{ab}} + \sum_{a \in C} \sum_{p \in S} \frac{Z_a Q_p}{R_{ap}} + \sum_{p > q \in S} \frac{Q_p Q_q}{R_{pq}}, \quad (1)$$

in which i and j label the electrons in cluster C, a and b label the nuclei in cluster C, while p and q label the positions of point charges in the surroundings S. T_i is the electronic kinetic energy of electron i . Z_a refers to nuclear charge, and r refers to distance. So $-Z_a/r_{ia}$ is the electron–nuclear attraction in cluster C, while $-Q_p/r_{ip}$ corresponds to the interaction between the point charge Q_p in the surroundings S and the electron i in cluster C. The value of point charge Q_p modifies the core Hamiltonian of the cluster in terms of one-electron integrals. $-\sum_{i \in C} \sum_{p \in S} Q_p/r_{ip}$. Q_p is a predetermined parameter entering the ab initio calculation. Normally, nominal values are employed; however, it is clear that different Q_p of the surroundings S will produce different Φ_C of cluster C; the requirement for consistence between the cluster and its surroundings should be met.

If atom a of cluster C is equivalent to point p of the surroundings S in the bulk solid, it is anticipated that the charge on point p should be equal to the charge on atom a .

$$Q_p = Q_a. \quad (2)$$

Therefore one needs to reach the charge consistence [35, 36]. That is, the charges used for embedding should be consistent with the charges derived from the wave functions of the embedded cluster.

Suppose point p is equivalent to atom a , and point q is equivalent to atom b , then it is required that

$$R_{ab} = R_{pq}. \quad (3)$$

When PCs p and q are fixed at the geometry of the bulk solid, the optimized geometry for cluster C could be in accordance with that for the surroundings S after choosing suitable values of Q_p . We call this potential consistence [35, 36], i.e., the interaction potential produced by PCs is balanced by that produced by the equivalent atoms at the equilibrium lattice position (R_c).

Taking the dipole moment as a criterion and assuming

$$|\mu_S| = |\mu_C|, \quad (4)$$

we need to reach the dipole moment consistence [35, 36] to determine Q_p .

In the literature, there are some other ways to determine the values of PCs. For example, the values of surrounding PCs are reduced from nominal values of 2 to 1.5 for MgO(100) so as to make the calculated CO vibrational frequency agree better with experimental results for CO/MgO [37]; the PCs are optimized so as to reproduce the exact Madelung potential in a rather large region of the space surrounding the cluster model [38]; the PCs are fitted to the calculated dipole moment from the band structure approach; etc. Taking MgO and NiO as examples, we have investigated the influence of the surrounding PCs on the calculated electronic properties of the embedded cluster [35, 36]. Charge consistence potential, and dipole moment consistence have been examined. It has been shown that the basic difference between a PC and a real atom lies in the fact that a real atom possesses a continuous distribution of charge density, while a PC does not. Therefore, we have tried to spherically expand the PC, so as to furnish it with a continuous distribution of charge density. It is found that charge density consistence enables a better cluster modeling. The spherical expansion of the PC Q_p can be processed as follows [35, 36].

The spherical function is

$$\varphi_s(r) = \left(\frac{2\alpha}{\pi} \right)^{3/4} \exp(-\alpha r^2). \quad (5)$$

We then have a spherically expanded PC with charge density $q_p(r)$ in the form of

$$q_p(r) = Q_p [\varphi_s(r)]^2, \quad (6)$$

$$Q_p = \int q_p(r) d\tau \text{ or } dv \quad (7)$$

From Eqs. (5–7), it can be easily deduced that the orbital exponent α is inversely proportional to the square of orbital radius $\langle r \rangle$. Substituting the orbital radius $\langle r \rangle$ with the ion radius $\langle R \rangle$, we find that $\langle R \rangle$ and the exponent α obey the relation

$$\alpha = \frac{3}{2\langle R \rangle^2}, \quad (8)$$

5 Embedded cluster modeling of MgO(100) and CO/MgO(100) adsorption systems

The interaction of a CO molecule with an MgO(100) surface has been the subject of intensive studies both experimentally and theoretically [13, 16–18, 23, 37, 39–48]. This system has been extensively used as a test case of theoretical models of chemisorption on ionic surfaces. The striking discrepancy between theory and experiment lies in the CO binding energy to the surface. The experimental heat of adsorption was initially reported to be rather low, only 0.15–0.17 eV [39, 40]; while later experiments gave a much higher value of 0.43–0.45 eV [41, 42]. Pacchioni and coworkers reported a RHF binding energy of 0.24 eV. This was obtained with $[\text{MgO}_5]^{8-}$ clusters embedded in an array of PCs [16, 17]. With the cluster model extended to $(\text{MgO})_{21}$ and with

the basis set superposition errors (BSSE) correction included, the binding energy was reduced to 0.08 eV [46]. Local density functional theory with embedded $[\text{MgO}_5]^{8-}$ predicted an extremely high value of the binding energy (1.20 eV [37, 46]), while the larger cluster model, $(\text{MgO})_{25}$, with gradient correction led to a binding energy of only 0.09 eV [44]. The best quantum chemical cluster model calculations to date are those of Nygren and coworkers [13, 45]. After the employment of accurate embedding techniques with full account of the crystal potential and a high-level treatment of dynamical correlation using large basis sets, the BSSE-corrected binding energy for CO adsorbed on MgO(100) regular sites was found to be 0.08 eV [13, 45]. These theoretical results have led to the conclusion that the binding energy was overestimated in experiments due to the high concentration of defect sites in the MgO slab samples [18, 44, 45]. In this report, we will discuss the CO orientation with the C atom perpendicular to the Mg cation of the regular site on MgO(100). We focus on the methods to describe the influence of the surroundings on the calculated electronic properties of $(\text{MgO})_x$ and $\text{CO}/(\text{MgO})_x$.

The fivefold coordinated Mg^{2+} adsorption site on MgO(100) is represented by a set of stoichiometric clusters of two layers (Fig. 2). These clusters are $(\text{MgO})_5(5, 5)$, $(\text{MgO})_5(9, 1)$, $(\text{MgO})_9(9, 9)$, $(\text{MgO})_{13}(13, 13)$, and $(\text{MgO})_{13}(21, 5)$. (The numbers of atoms in each layer are given in parentheses.) The reason we chose these clusters lies in that they all possess the correct local C_{4v} symmetry. The molecular clusters $(\text{MgO})_x$ are embedded in the symmetric array of $(11 \times 11 \times 6) - 2 \times \text{PCs}$. An unreconstructed MgO(100) surface is assumed with an Mg—O distance of 2.105 Å [25]. In the first embedding scheme, the nominal values of ± 2 a.u. are employed. (This kind of model is called the NPC model.) In the second embedding scheme, the nearest positive PCs are replaced by a total ion potential (TIP model [49, 50]) of Mg^{2+} , which prevents the electronic charge distribution of O^{2-} ions from polarizing too far toward the $+2$ PC neighbors. In the third embedding scheme, we expand the nearest negative PC spherically (SPC model) to account for the finite size

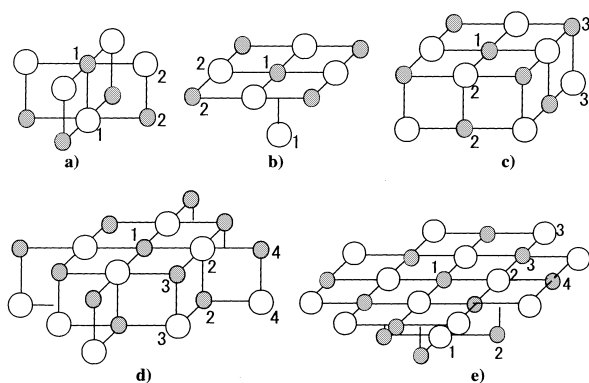


Fig. 2a–e. Cluster models for the five-fold coordinated Mg^{2+} adsorption site on MgO(100). **a** $(\text{MgO})_5(5, 5)$; **b** $(\text{MgO})_5(9, 1)$; **c** $(\text{MgO})_9(9, 9)$; **d** $(\text{MgO})_{13}(13, 13)$; **e** $(\text{MgO})_{13}(21, 5)$. Filled circles stand for Mg cations, and open circles for O anions. The numbers nearby the circles label the types of ions

effect of the lattice ions. The embedding spherical charges have been self-consistently determined to be around the values of ± 1.6 a.u. Assuming the quantum effects, i.e., the exchange and core-orthogonality effects, are similar to those in the TIP model, the same pseudopotential is employed to replace the nearest positive PCs with only modification of the Coulomb terms for cations of $q = +1.6$ a.u.

The results of $(\text{MgO})_x$ cluster modeling of the MgO(100) surface with various kinds of models are presented in Table 3. The calculated properties include Mulliken charges, q , on different types of ions, the highest occupied molecular orbital (HOMO) energy level in eV, and the energy gap, ΔG , between the HOMO and the lowest unoccupied molecular orbital (LUMO). The main results can be summarized as follows.

1. In MgO bulk solid, the charges on Mg or O should all be the same and the ratio between the absolute charge on Mg and that on O should be 1:1. For bare-cluster models, this stoichiometry as well as the neutrality requirement is only roughly fulfilled by the cubic $(\text{MgO})_9(9, 9)$ cluster. This is not surprising as we recall that the topologic parameters N and β predict that the cubic model is the best model and those models with ions of coordination numbers less than 2 should be avoided. Larger clusters, $(\text{MgO})_{13}$, do not seem to provide better models for MgO solid or surface than $(\text{MgO})_9$ does. Indeed, β_d shows a local minimal at $x = 9$.

2. In the cluster modeling of surfaces, it is quite common to build up the model in the shape of an inverse pyramid like $(\text{MgO})_5(9, 1)$ or $(\text{MgO})_{13}(21, 5)$. Mulliken charges seem to provide a simple, yet useful tool for measuring the reliability of a cluster model. The charge on the singly coordinated O atom of bare $(\text{MgO})_5(9, 1)$ is significantly low, while the charge on the central Mg cation of bare $(\text{MgO})_{13}(21, 5)$ is extremely high. This may be simply attributed to the drawback of Mulliken population analysis. However, we argue that this would be an indication for a poor geometry of the cluster compared to that of the solid or the surface. Both these clusters possess the lowest calculated energy gaps among this set of clusters. In bare $(\text{MgO})_5(9, 1)$, the dangling bonds lead to a too high-lying HOMO, which brings about a too low ΔG , while in bare $(\text{MgO})_{13}(21, 5)$, the small ΔG results from the overstabilized LUMO. Compared with the experimental ΔG value of 7.8 eV [51], the result of 8.56 eV calculated from cubic $(\text{MgO})_9(9, 9)$ within bare-cluster models seems reasonable.

3. Embeddings not only make $(\text{MgO})_x$ closer to the bulk solid, but also result in better similarity among clusters of different size and shape. The ionicities of these clusters are generally increased, while these clusters are stabilized with the HOMOs moving to lower energy. In general, the ΔG s calculated with the SPC model are in better agreement with the experimental value of 7.8 eV [51]. It is worth noting that the smallest change in the charge distribution upon embedding occurs on $(\text{MgO})_9$. This suggests that cluster-lattice interaction is weakest for $(\text{MgO})_9$ among this series of cluster models, and that the bare-cluster model, if properly chosen, may provide a reasonable description of the solid.

Table 3. $(\text{MgO})_x$ cluster modeling of the $\text{MgO}(100)$ surface^a

| | Bare | NPC | TIP | SPC |
|----------------------------|--------|--------|--------|--------|
| $(\text{MgO})_5(5,5)$ | | | | |
| $q(\text{Mg1})$ | 1.564 | 0.790 | 1.151 | 1.269 |
| $q(\text{Mg2})$ | 0.697 | 1.692 | 1.810 | 1.623 |
| $q(\text{O}_1)$ | -1.310 | -1.536 | -1.597 | -1.482 |
| $q(\text{O}_2)$ | -0.761 | -1.505 | -1.699 | -1.570 |
| HOMO (eV) | -7.54 | -11.5 | -9.59 | -8.56 |
| ΔG (eV) | 5.30 | 11.3 | 11.3 | 7.33 |
| $(\text{MgO})_5(9,1)$ | | | | |
| $q(\text{Mg1})$ | 1.055 | 0.457 | 1.553 | 1.658 |
| $q(\text{Mg2})$ | 0.990 | 1.783 | 1.694 | 1.555 |
| $q(\text{O}_1)$ | -0.313 | -1.520 | -1.911 | -1.863 |
| $q(\text{O}_2)$ | -1.175 | -1.517 | -1.605 | -1.504 |
| HOMO (eV) | -3.52 | -11.4 | -9.84 | -7.60 |
| ΔG (eV) | 3.01 | 11.6 | 11.7 | 7.43 |
| $(\text{MgO})_9(9,9)$ | | | | |
| $q(\text{Mg1})$ | 1.209 | 1.250 | 1.376 | 1.400 |
| $q(\text{Mg2})$ | 1.215 | 1.578 | 1.626 | 1.531 |
| $q(\text{Mg3})$ | 1.241 | 1.385 | 1.630 | 1.525 |
| $q(\text{O}_1)$ | -1.372 | -1.465 | -1.564 | -1.509 |
| $q(\text{O}_2)$ | -1.271 | -1.405 | -1.496 | -1.438 |
| $q(\text{O}_3)$ | -1.144 | -1.505 | -1.714 | -1.590 |
| HOMO (eV) | -8.77 | -12.0 | -9.57 | -9.50 |
| ΔG (eV) | 8.56 | 12.8 | 11.4 | 8.91 |
| $(\text{MgO})_{13}(13,13)$ | | | | |
| $q(\text{Mg1})$ | 1.563 | 1.330 | 1.343 | 1.329 |
| $q(\text{Mg2})$ | 1.341 | 0.922 | 1.522 | 1.522 |
| $q(\text{Mg3})$ | 0.901 | 1.533 | 1.772 | 1.649 |
| $q(\text{Mg4})$ | 0.695 | 1.864 | 1.680 | 1.504 |
| $q(\text{O}_1)$ | -1.348 | -1.444 | -1.544 | -1.488 |
| $q(\text{O}_2)$ | -1.322 | -1.408 | -1.408 | -1.366 |
| $q(\text{O}_3)$ | -1.049 | -1.401 | -1.719 | -1.604 |
| $q(\text{O}_4)$ | -0.620 | -1.482 | -1.797 | -1.666 |
| HOMO (eV) | -7.82 | -11.6 | -9.60 | -8.74 |
| ΔG (eV) | 5.43 | 11.8 | 11.2 | 8.59 |
| $(\text{MgO})_{13}(21,5)$ | | | | |
| $q(\text{Mg1})$ | 2.407 | 1.390 | 1.301 | 1.417 |
| $q(\text{Mg2})$ | 0.562 | 1.925 | 1.885 | 1.753 |
| $q(\text{Mg3})$ | 0.891 | 1.018 | 1.465 | 1.425 |
| $q(\text{Mg4})$ | 1.200 | 1.418 | 1.511 | 1.328 |
| $q(\text{O}_1)$ | -1.323 | -1.484 | -1.589 | -1.484 |
| $q(\text{O}_2)$ | -1.307 | -1.407 | -1.407 | -1.354 |
| $q(\text{O}_3)$ | -0.808 | -1.465 | -1.690 | -1.568 |
| HOMO (eV) | -8.05 | -11.3 | -9.47 | -9.20 |
| ΔG (eV) | 3.58 | 11.5 | 11.6 | 7.96 |

^a RHF calculations with Gaussian 94[25]. The basis sets are 6-31G[25]

4. When $(\text{MgO})_x$ clusters are embedded in PCs, the atoms in the first layer become surface atoms of $\text{MgO}(100)$. These atoms are all fivefold coordinated, while the other atoms are sixfold coordinated, partly by PCs and partly by real atoms. There is evidence that the most stable $\text{MgO}(100)$ surface does not differ very much from bulk MgO [52]. However, in bare $(\text{MgO})_x$ clusters, the peripheral atoms possess lower charges owing to lower coordination numbers, while in embedded clusters, these atoms acquire higher values of charges due to the direct contact with PCs. The charge difference between a peripheral atom and an inner atom of a cluster model clearly shows the difference between a real ion and a PC. Taking $(\text{MgO})_5(5, 5)$ as an example, the charge difference between $q(\text{Mg1})$ and $q(\text{Mg2})$ is 0.90 for the NPC model, 0.66 for the TIP model, and 0.35 for the SPC model. Along this series, the decrease in charge difference should imply an improvement in the description of the surroundings. It is interesting to note that the

charge differences among various kinds of O anions are smaller than those of Mg cations. This may suggest that the compact Mg cation is reasonably approximated by a positive PC, and that a better description of the O anion should take into account the finite size of the anions. Here we recall the topological parameter N_a introduced in Sect. 3. A smaller N_a , indicating a smaller number of PCs in direct contact with the cluster atoms, would infer a better embedded cluster model.

The results for $\text{CO}/(\text{MgO})_x$ calculated with different models are listed in Table 4. The Mg—C distance was optimized for a fixed C—O bond length of $r(\text{C—O}) = 1.104 \text{ \AA}$ with the positions of substrate atoms and PCs always being fixed in the crystalline structure of MgO . The equilibrium bond distance, $r_e(\text{Mg—C})$ was determined by a fourth-degree polynomial fit to five $r(\text{Mg—C})$ points around the minimum of the corresponding potential energy curve. The bonding energy D_e was calculated from the total energy of the

Table 4. Comparison of the results for the CO/MgO(100) adsorption system^a

| | Bare | NPC | TIP | SPC | $\Delta r_e/\Delta D_e$ ^b |
|---------------------------------------|-------|-------|-------|-------|--------------------------------------|
| CO/(MgO) ₅ (5,5) | | | | | |
| $r_e(\text{Mg}-\text{C})(\text{\AA})$ | 2.451 | 2.528 | 3.386 | 3.109 | 0.935 |
| D_e (eV) | 0.310 | 0.422 | 0.059 | 0.062 | 0.363 |
| CO/(MgO) ₅ (9,1) | | | | | |
| $r_e(\text{Mg}-\text{C})(\text{\AA})$ | 2.661 | 2.348 | 3.078 | 3.276 | 0.928 |
| D_e (eV) | 0.077 | 1.059 | 0.037 | 0.048 | 1.022 |
| CO/(MgO) ₉ (9,9) | | | | | |
| $r_e(\text{Mg}-\text{C})(\text{\AA})$ | 3.241 | 2.777 | 3.187 | 3.248 | 0.147 |
| D_e (eV) | 0.045 | 0.183 | 0.050 | 0.060 | 0.138 |
| δr_e ^c | 0.790 | 0.429 | 0.308 | 0.167 | – |
| δD_e ^c | 0.265 | 0.876 | 0.022 | 0.014 | – |

^a RHF calculations with Gaussian94 [25]. The basis sets for (MgO)_x are 6-31G[25]. The CO basis sets are (9s, 5p, 1d)/[4s, 3p, 1d] [50]

^b Variations of the calculated properties with the embedding schemes

^c Variations of the calculated properties with cluster size and shape

free system the minus energy of the interacted system. For CO/(MgO)₅(5,5), the bare-cluster model predicts a $r_e(\text{Mg}-\text{C})$ of 2.451 Å and a D_e of 0.310 eV. The adsorption bond is obviously overestimated by this model. The NPC model gives essentially the same results with $r_e(\text{Mg}-\text{C})$ somewhat lengthened and D_e (eV) increased. The results from the TIP and SPC models are significantly different. CO interaction with MgO(100) regular sites is shown to be very weak with $r_e(\text{Mg}-\text{C})$ larger than 3.0 Å and D_e around 0.06 eV. These results are in good agreement with the most recent and most accurate calculations [45]. For CO/(MgO)₅(9, 1), the results from the bare-cluster model and the NPC model are quite contrary. The bare-cluster model gives a longer $r_e(\text{Mg}-\text{C})$ with a smaller D_e , while the NPC model predicts a $r_e(\text{Mg}-\text{C})$ which is too short and a D_e which is too large. Enlarging the cluster size from (MgO)₅ to (MgO)₉(9, 9) improves the calculation results. The bare-cluster model of (MgO)₉(9, 9) gives results which are quite similar to those of the TIP and SPC models. We do not go into details of CO/(MgO)₁₃ cluster models, as we believe that (MgO)₁₃ behaves no better than (MgO)₉.

It is interesting to see how the calculated adsorption properties vary with the methods to describe the surroundings as well as with the size and shape of the clusters. For CO/(MgO)₅(5, 5) models, the different descriptions of the surroundings result in variations in r_e of 0.935 Å and in D_e of 0.363 eV, while for CO/(MgO)₅(9, 1), Δr_e is 0.928 Å and ΔD_e is 1.022 eV. These variations are greatly reduced to $\Delta r_e = 0.471$ Å and $\Delta D_e = 0.138$ eV in CO/(MgO)₉(9, 9). For the bare-cluster models of different sizes and shapes, the calculated r_e have a variance of 0.790 Å and the D_e have a variance of 0.265 eV. The results of the bare-cluster models are quite size-dependent. Only cubic (MgO)₉(9, 9) provides good modeling of a solid. For the NPC models, δr_e and δD_e are 0.429 Å and 0.876 eV, respectively. This seems to support the argument that the simple PC model does not always lead to improved modeling of the solid [47, 54]. The TIP model clearly reduces this variance. The variations of r_e and D_e are 0.308 Å and 0.022 eV, respectively. The δr_e and δD_e are further decreased to 0.167 Å and 0.014 eV, respectively, in the SPC model. From

the inspection of the changes in Δr_e , ΔD_e , δr_e , and δD_e , we may conclude that a better cutout cluster, which interacts less with the surroundings, would depend less on the embedding scheme, while a better description of the surroundings would improve the quality of the cutout cluster. The effect of the surroundings on the calculated adsorption properties is not only through the long-range Coulomb interactions on the adsorbate, but also through the influence of the properties of the substrate cluster.

6 Concluding remarks

A bulk solid can be regarded as the sum of two fragments. One is a cutout cluster which will be explicitly treated in quantum chemical calculations, the other is the surroundings of the cutout cluster. Accordingly, in order to establish a reasonable embedded-cluster model, one has to answer two questions: (1) how to cut out a cluster and (2) how to suitably account for the cluster-lattice interaction. For the first question, we have proposed three principles, namely, a neutrality principle, a stoichiometry principle and a coordination principle, according to which a neutral, stoichiometrical cutout cluster with the minimum number of dangling bonds is preferred. We have shown good correlation between the topological parameters N (N_c , N_d , or N_a) and β (β_c , β_d , or β_a), and the stability of clusters. We believe that these topological parameters provide meaningful criteria to cut out a better cluster model without paying for the high cost of detailed preliminary calculations. A good cutout cluster is itself not only a good bare-cluster model, but also a suitable starting point for embedding or saturation. For the second question, we have demonstrated how the calculated electronic properties of the substrate clusters and the adsorption properties vary with the ways to describe the surroundings. It is shown that a better cutout cluster, which interacts less with the surroundings, would depend less on the embedding scheme, while a better description of the surroundings would improve the quality of the cutout cluster. The SPC model provides the most stable modeling of the oxide surface as well as of adsorption on the surface.

Recently, we have studied several representative chemisorption systems, for example, CO/MgO, O/MgO, CO/ZnO, O/ZnO, H₂/ZnO, and H₂/TiO₂, with the SPC cluster model method and have investigated the effects of size and symmetry of the PC array, the size dependence of the cluster model, the basis sets, and electron correlation on the theoretical description of adsorptive bonding. Based on the findings in this paper and those presented elsewhere, the main points of our so-called SPC cluster model can be summarized as follows: a stoichiometric cutout cluster with the fewest dangling bonds embedded in a symmetric PC array, and spherically expanded PC surroundings with charges being self-consistently determined. Our case studies of chemisorption on metal oxides with different degrees of ionicity demonstrated the efficiency of the SPC cluster model.

Acknowledgements. This project was supported by the National Natural Science Foundation of China, the Doctoral Project Foundation of the State Ministry of Education of China, the Fok Ying Tung Education Foundation, and the Japan Society for the Promotion of Science.

References

- Kung HH (1989) Transition metal oxides: surface chemistry and catalysis. Amsterdam, Elsevier
- Freund H-J, Umbach E (eds) (1994) Adsorption on ordered surfaces of ionic solids and thin films. Springer, Berlin Heidelberg New York
- Pacchioni G, Bagus PS (eds) (1992) Cluster models for surface and bulk phenomena, NATO ASI Series B Vol 283. Plenum, New York
- Colbourn EA (1992) Surf Sci Rep 15: 281
- Jug K, Geudtner G, Bredow T (1993) J Mol Catal 82: 171
- Sauer J (1989) Chem Rev 89: 199
- Pisani C, Cora F, Nada R, Orlando R (1994) Comput Phys Commun 82: 139
- Lopez-Moraza S, Pascual JL, Barandiaran Z (1995) J Chem Phys 103: 2117
- Mejias JA, Fernandez-Sanz J (1995) J Chem Phys 102: 327
- Eichler U, Kolmel CK, Sauer J (1996) J Comput Chem 18: 463
- Maseras F, Morokuma K (1995) J Comput Chem 16: 1170
- Field MJ, Bash PA, Karplus M (1990) J Comput Chem 11: 700
- Nygren MA, Pettersson LGM, Barandiaran Z, Sejio L (1994) J Chem Phys 100: 2010
- Lu X, Xu X, Wang NQ, Zhang QE, Ehara M, Nakatsuji H (1998) Chem Phys Lett 291: 445
- Lu X, Xu X, Wang NQ, Zhang QE (1998) Chem J Chin Univ 19: 783
- Pacchioni G, Cogliandro G, Bagus PS (1992) Int J Quantum Chem 42: 1115
- Pacchioni G, Cogliandro G, Bagus PS (1991) Surf Sci 255: 344
- Mejias JA, Marquez AM, Fernandez Sanz J, Fernandez-Garcia M, Ricart JM, Sousa C, Illas F (1995) Surf Sci 327: 59
- Sangster MJL, Peckham G, Saunderson DH (1970) J Phys C 3: 1026
- Sasaki S, Fujina K, Takeuchi Y, Sadanaga R (1980) Acta Crystallogr Sect. A 36: 904
- Birkenheuer U, Boettger JC, Rosch N (1994) J Chem Phys 100: 6826
- Berrondo M, Rivas-silva JF (1996) Int J Quantum Chem 57: 1115
- Neyman KM, Rosch N (1993) Surf Sci 297: 223
- Xu X, Lu X, Wang NQ, Zhang QE (1995) Chem Phys Lett 235: 541
- Wyckoff RWG (1963) Crystal structures, vol 1. Interscience, New York
- Jug K, Geudtner G (1993) Chem Phys Lett 208: 537
- Frisch MJ, Trucks GW, Schlegel HB, Gill PMW, Johnson BG, Robb MA, Cheeseman JR, Keith T, Petersson GA, Montgomery JA, Raghavachari K, Al-Laham MA, Zakrzewski VG, Ortiz JV, Foresman JB, Peng CY, Ayala PY, Chen W, Wong MW, Andres JL, Replogle ES, Gomperts R, Martin RL, Fox DJ, Binkley JS, Defrees DJ, Baker J, Stewart JP, Head-Gordon M, Gonzalez C, Pople JA (1995) Gaussian 94, Gaussian, Pittsburgh, Pa
- Stevens WJ, Basch H, Krauss M (1984) J Chem Phys 81: 6026
- Lu X, Xu X, Wang NQ, Zhang QE (1998) Chin Chem Lett 9: 545
- Lu X, Xu X, Wang NQ, Zhang QE (1999) Chem Phys Lett (in press)
- Lu X, Xu X, Wang NQ, Zhang QE (1999) J Phys Chem B (in press)
- Beck AD (1993) J Chem Phys 98: 5648
- Lee C, Yang W, Parr RG (1988) Phys Rev B 37: 785
- Kaplan IG (1986) Theory of Molecular Interactions. Elsevier, Amsterdam, p20
- Xu X, Nakatsuji H, Ehara M, Lu X, Wang NQ, Zhang QE (1998) Sci China Ser B 41: 113
- Xu X, Nakatsuji H, Ehara M, Lu X, Wang NQ, Zhang QE (1998) Chem Phys Lett 292: 282
- Neyman KM, Rosch N (1992) Chem Phys 168: 267
- Sousa C, Casanovas J, Rubio J, Illas F (1993) J Comput Chem 14: 680
- Paukshitis EA, Soltanov RI, Yurchenko NE (1981) React Kinet Catal Lett 16: 93
- Furuyama S, Fujii H, Kawamura M, Morimoto T (1978) J Phys Chem 82: 1028
- Henry CR, Chapon C, Duriez C (1991) J Chem Phys 95: 700
- He JW, Estrada CA, Corneille JS, Wu MC, Goodman DW, (1992) Surf Sci 261: 164
- Scarano D, Spoto G, Bordiga S, Coluccia S, Zecchina A (1992) J Chem Soc Faraday Trans 88: 291
- Neyman KM, Ruzankin S Ph, Rosch N (1995) Chem Phys Lett 246: 546
- Nygren MA, Pettersson LGM (1996) J Chem Phys 105: 9339
- Pacchioni G, Neyman KM, Rosch N (1994) J Electron Spectrosc Relat Phenom 96: 13
- Pacchioni G, Ferrari AM, Marquez AM, Illas F (1997) J Comput Chem 18: 617
- Pascual JL, Pettersson LGM (1997) Chem Phys Lett 270: 351
- Winter NW, Pitzer RM, Temple DK (1987) J Chem Phys 86: 3549
- Stevens W, Basch H, Krauss J (1984) J Chem Phys 81: 6026
- Roessler DM, Walker WC (1967) Phys Rev 159: 733
- Martin AJ, Bilz H (1979) Phys Rev B 19: 977
- van Duinveldt FB (1971) IBM Research Report No RJ945
- Pelmenschikov AG, Morosi G, Gamba A, Coluccia S (1995) J Phys Chem 99: 15018